

Development and Experimental Validation of a CFD Pulse-tube Design Tool

*CEC Timmerhaus Scholarship Interim Progress Report
FY-2008*

Ryan Taylor
University of Wisconsin-Madison

Introduction

The pulse-tube cryocooler (PTC) provides a reliable, compact, and efficient method for producing cryogenic refrigeration. In many ways, the PTC represents a straightforward extension of the more mature Stirling cryocooler. The key difference is the replacement of the displacer in the Stirling cryocooler with the pulse-tube in a PTC. The function of the displacer is to transmit power from the cold end to the warm end of the machine. The pulse-tube performs a similar function in the PTC; however, while the behavior of a displacer is easily controlled, the performance of the pulse-tube in a PTC is more complex because the gas that acts as a compliant piston is less well controlled. The efficiency of the pulse-tube (i.e., its ability to convert acoustic power into useful cooling) may be limited by several, relatively complex loss mechanisms that are not present in a Stirling cryocooler.

The overall objective of this project is to carry out fundamental work that will enable the deployment of high efficiency pulse-tube cryocoolers by developing an experimentally verified and powerful CFD model that can be applied to the design of efficient pulse-tubes and transitions. The specific objectives of this work are the development of the CFD design model for pulse-tube/flow transition behavior, verify the developed model for numerical convergence and validate it against experimental data taken in collaboration with the Cryogenic Technologies Group at NIST, and to generate design charts for 4K pulse-tube cryocoolers.

Progress

During the 2008 fiscal year, the following research progress was made:

1. finalized development of the CFD model with addition of real gas property routines,
2. finalized the experimental validation methodology,
3. performed the thermal bus calibration for the test facility,
4. performed the mass flow calibrations for the anticipated operating conditions, and
5. performed initial characterization of a regenerator including experimental uncertainty.

These topics are discussed in more detail in the remainder of this report.

1. Background

The CFD design model developed as part of this project is focused on the pulse-tube and flow transitioning components within a PTC (rather than simulating the entire PTC); this approach more efficiently provides useful results by focusing on the areas of the PTC where the multi-dimensional and complex flow occurs and results in refrigeration loss. The CFD model is a two-dimensional (2-D) axi-symmetric model of the pulse-tube and flow transitioning components that are implemented in the commercial CFD solver package FLUENT. The notable features of this model include:

1. the ability to model the wire mesh screens that are typically utilized to control the flow in flow transitions through the use of a porous media model that employs empirical data to represent the inertial and viscous flow resistances in the axial and radial directions,
2. the simulation of turbulence that is present due to the high velocity flows at the warm end of the system using an appropriate turbulence model,

3. the ability to model two working fluids, ^4He and ^3He , via the use of the ideal gas equation of state or by coupling the NIST REFPROP package (which in standard form does not include helium 3 properties) to the CFD simulation, and
4. simulation times that range from 6 to 48 hours (i.e., days) compared to other models of the entire PTC that require simulation times on the order of weeks to reach cyclic steady state.

The outputs from the model are quantitative in nature and the quantities reported to the user include: (*primary*) the pulse-tube energy flow and the acoustic power flow and (*secondary*) the effectiveness of the pulse-tube component with respect to converting acoustic power into useful cooling as well as the delineated losses associated with conduction, shuttle heat loss, and turbulence.

1. Real Gas Property Routines

Previous work related to the CFD model development has relied upon the assumption that the helium working fluid was an ideal gas. While this is a valid assumption for operational temperatures above 40K where the compressibility is approximately 1, this assumption no longer holds for PTC's which have cold end temperatures over the range of 4.2-40K. As a result, it was necessary to incorporate real gas properties into the model simulations. This task was facilitated via the use of the commercially available property package from NIST called REFPROP. The FLUENT CFD code allows for this set of property routines to be utilized with the CFD code such that at each computation, the REFPROP routines are called by the model to provide the actual real gas properties. In addition to being able to now model ^4He as a real gas, the ability to model ^3He has also been added. The reason for addition of this fluid is that the current state of cryocooler research is aimed at utilizing ^3He at 4.2K to improve the thermodynamic efficiency of PTC's.

2. Experimental Measurement Methodology

In order for the CFD model to be accepted and applied with confidence to a design problem, it must be experimentally verified by via comparison to experimental data. An energy balance applied to the cold heat exchanger in a PTC at steady state (Figure 1) leads to:

$$\dot{E}_{REG,c} + \dot{Q}_{net} = \dot{E}_{PT,c} \quad (1)$$

where $\dot{E}_{REG,c}$ is the cycle average regenerator energy flow term, \dot{Q}_{net} is the cycle average net cooling power, and $\dot{E}_{PT,c}$ is the cycle average energy flow through the pulse-tube and flow transitioning components. The regenerator energy flow term is also called the regenerator loss and it is the manifestation of the ineffectiveness of the regenerator; gas moving into the cold heat exchanger from the regenerator tends to be warmer than gas flowing into the regenerator from the cold heat exchanger. The pulse-tube energy flow term is the gross cooling power available for the PTC and is the manifestation of the expansion process that occurs within the pulse-tube; gas flowing into the cold heat exchanger from the pulse-tube tends to be colder than gas flowing into the pulse-tube from the cold heat exchanger. Also illustrated in Figure 1 (but not part of the energy balance) is the cycle average acoustic power flow at the cold end of the system. The acoustic power is calculated according to:

$$\dot{W}_{PV,c} = \langle P\dot{V} \rangle = \frac{1}{\tau} \int_0^{\tau} \int_0^R (\tilde{P}u) 2\pi r dr dt \quad (2)$$

where \tilde{P} is the dynamic pressure at the cold end and u is the velocity at the cold end.

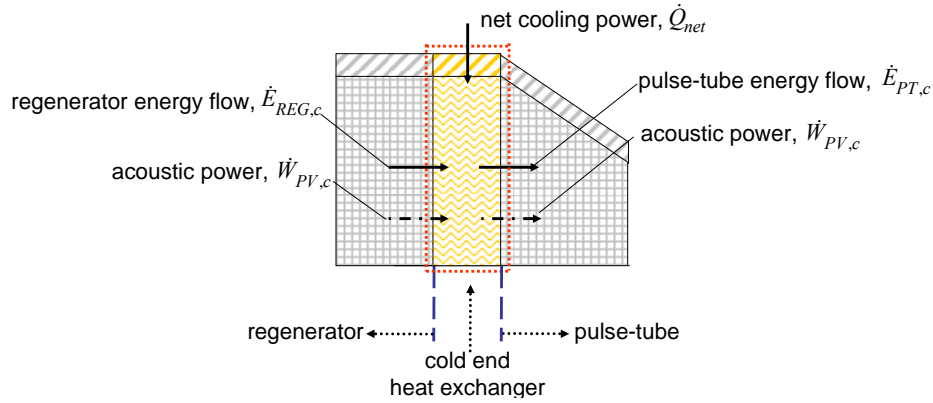


Figure 1: Illustration showing an energy balance applied to the cold heat exchanger in a PTC with delineation of the energy and power flows.

The acoustic power is not a thermodynamic energy flow but rather is the theoretical maximum rate of refrigeration which would be provided if the gas entering the pulse-tube were expanded reversibly against a piston. The value of $\dot{E}_{PT,c}$ can never exceed $\dot{W}_{PV,c}$, therefore the acoustic power is used by designers to predict the performance of the pulse-tube component. The ratio of $\dot{E}_{PT,c}$ to $\dot{W}_{PV,c}$ is referred to as the pulse-tube efficiency and the difference between $\dot{W}_{PV,c}$ and $\dot{E}_{PT,c}$ is referred to as the pulse-tube loss. The pulse-tube loss is the most important quantity predicted by the CFD model and therefore both $\dot{W}_{PV,c}$ and $\dot{E}_{PT,c}$ must be experimentally measured in order to verify the CFD model. However, the quantity that is most directly measurable for a PTC is the net cooling power. According to Eqn. (1), the net cooling power is equal to the pulse-tube energy flow less the regenerator energy flow (i.e., the "regenerator loss"). Therefore, the regenerator energy flow must be separately measured in order to infer the pulse-tube energy flow from the net cooling power. The acoustic power must also be measured in order to determine the efficiency of the pulse-tube.

Based on this discussion, the quantities that must be measured separately include the regenerator loss, the net cooling power, and the acoustic power flow; from these quantities, the pulse-tube energy flow and pulse-tube loss can be determined for validation. None of these energy flows are directly measurable and therefore it is necessary to develop an experimental methodology that allows these terms of interest to be computed based on other measurements. The experimental methodology is summarized below and discussed in more detail in the subsequent sections.

1. calibration of a thermal bus that allows for heat from/to the cold end to be measured.
2. calibration of a custom mass flow meter for use under oscillatory flow conditions at cryogenic temperatures.
3. measurement of the regenerator loss, independent of the pulse-tube component.
4. measurement of the net cooling power with a pulse-tube.
5. measurement of the acoustic power flow at the cold end of the system.

3. Bus Bar Calibration

A conductive path (referred to as the bus bar) is used to measure the rate of heat transfer between the experiment and an auxiliary source of cooling or heating, which is a commercial GM cryocooler outfitted with a heater system, as shown in Figure 2. The rate of heat transfer through the bus bar is related to the temperature difference across the bus bar via an in-situ calibration process. The warm end of the bus bar is eventually interfaced with the cold end of

the experimental system. The intercept temperature is set to a desired operating temperature using trim heaters on the cold stage of the commercial cryocooler. A second set of heaters (the calibration heaters) are installed at the warm end of the bar and provide a precisely measured amount of electrical heating that generates a finite temperature difference. The relationship between the temperature difference across the bus bar and the heater power conducted through it results in a calibration curve.

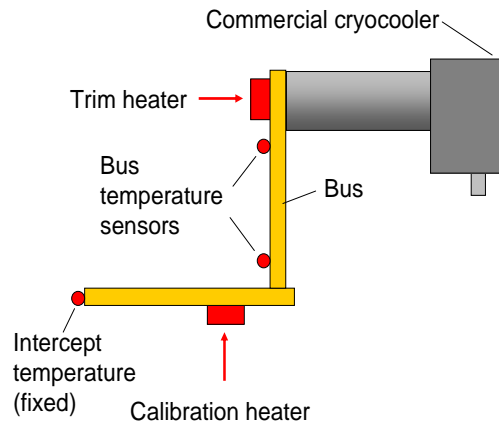


Figure 2: Schematic of the test set-up for calibration of the thermal bus bar.

This calibration curve has been generated over a range of heater power and at several warm end temperatures (note that by controlling the heaters placed on the commercial cryocooler it is possible to carry out these tests with the temperature of the warm end of the bus bar fixed). The bus bar calibration curve is shown in Figure 3 and is used in steps 3 and 4 of the experimental procedure to determine the regenerator loss and net cooling power, respectively, at a specific temperature. It should be noted that due to the highly non-linear thermal conductivity of the bus bar, the calibration must be repeated for all test temperatures of interest.

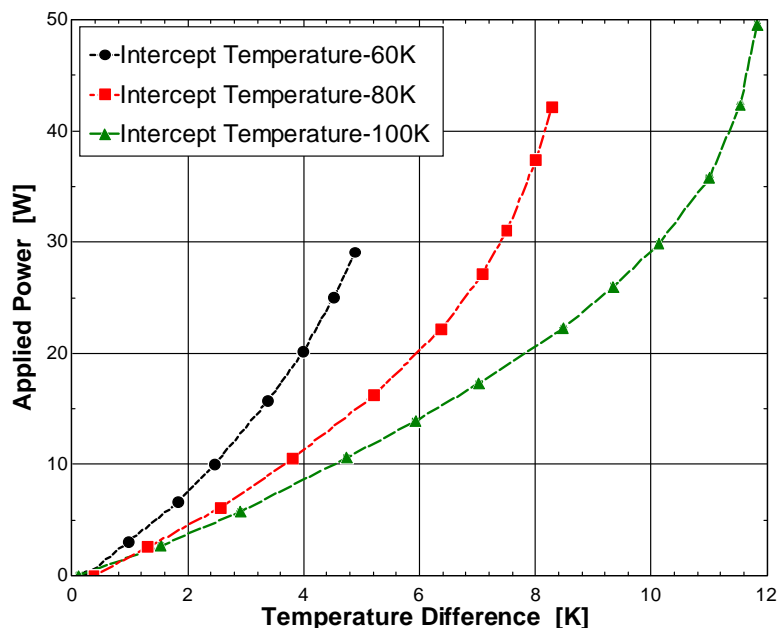


Figure 3: Plot showing the experimentally measured calibration curves for the bus bar utilized for measurement of the various energy flows for temperatures of 60, 80, and 100K.

4. Mass Flow Meter Calibration

It is difficult to measure the time resolved mass flow rate in a PTC due to the oscillatory, cryogenic nature of the flow. Instruments that are typically used, such as mass flow meters or

hot-wire anemometers tend to disturb the flow field as well as introduce unwanted dead volume in the system. Rawlins et al. (1993) has shown that the mass flow rate inside a PTC can be measured using specially designed hot-wire anemometers. However, discussions with the Cryogenic Technologies Group at NIST (who pioneered this measurement) indicate that hot-wire based mass flow rate measurements remain very difficult to make in the pulse-tube environment due to failures in the hot wire instrumentation. Also, these instruments do not work well below about 77 K due to the reduced electrical resistance of the hot wire that leads to an extremely large power dissipation required to generate a meaningful signal and therefore adds significant bias to the measurement.

An alternative method for measuring the mass flow rate at the cold end of the system correlates the instantaneous pressure drop across a small screen pack to the instantaneous mass flow rate. The calibration of the flow measuring device is accomplished by comparing the measured pressure difference across the flow resistance (under an oscillating flow condition) to the actual mass flow rate at the entrance of a reservoir of known volume, as shown in Figure 4. The flow resistance used for the experiment consists of a stack of copper mesh screens that serve the dual role of a thermal intercept (i.e., the screens are thermally connected to the bus bar that leads to the commercial cryocooler/heater system) as well as a flow measurement sensor.

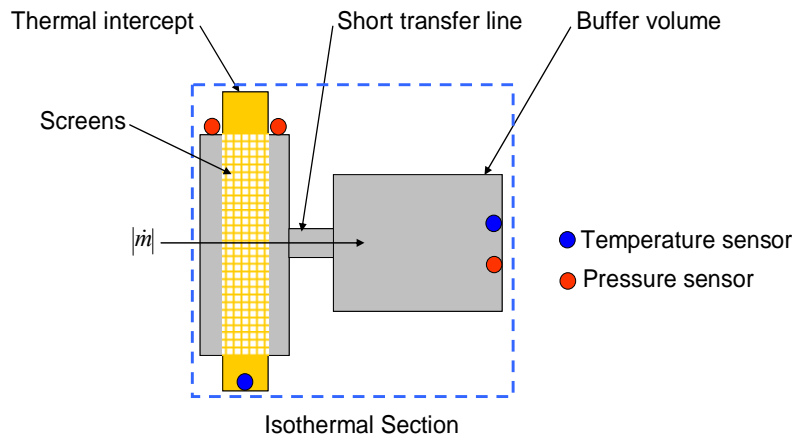


Figure 4: Schematic of the mass flow calibration test set-up.

The calibration of the amplitude of the pressure difference across the screens against the amplitude of the mass flow rate through the screens is carried out by installing the flow sensor on the cold end of the regenerator component and connecting it via a short transfer line to a reservoir of known volume, as shown in Figure 4. The GM cryocooler is used to cool the thermal sink, connecting line, and the reservoir volume to the same temperature. The gas temperature (reservoir temperature), pressure amplitude, and the volume of the reservoir are used to determine the magnitude of the mass flow rate $|\dot{m}_{res}|$ at the reservoir inlet according to Eqn. (3) (which assumes adiabatic behavior of the ideal gas in the reservoir),

$$|\dot{m}_{res}| = \frac{|\tilde{P}| V_{res}}{\gamma T_{res} R} \quad (3)$$

where V_{res} is the volume of the reservoir, T_{res} is the temperature of the reservoir gas measured via the reservoir wall temperature, and γ is the ratio of specific heat for the working fluid. The dead volume and flow resistance between the flow sensor and the reservoir volume is made as small as possible and therefore the mass flow rate entering the reservoir is very nearly equal to the mass flow passing through the flow sensor; the small difference is corrected for using an analytical model. The assumption of adiabatic conditions within the reservoir is justified by the fact that the size of the reservoir volume is orders of magnitude larger than the thermal

penetration depth into the gas. This implies that while there is some small heat transfer with the reservoir wall, the bulk of the gas in the reservoir experiences nearly an adiabatic process. The calibration of the mass flow meter at two mean pressures and an operating temperature of 80 K are shown in Figure 5.

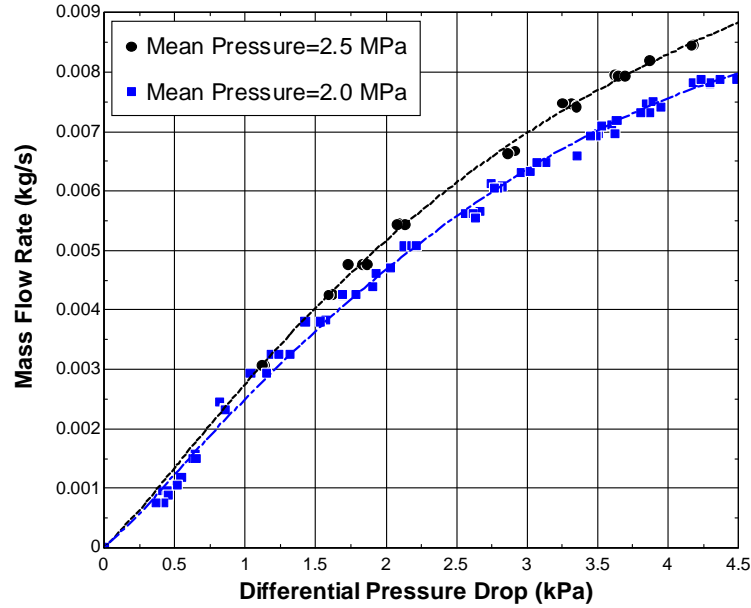


Figure 5: Plot showing the calibration data for the mass flow meter operating at 80K for mean pressures of 2.5 and 2.0 MPa.

5. Experimental Uncertainty and Initial Measurement Results

Experimental Uncertainty

As of present, only the measurement of the regenerator energy flow has been accomplished. As a result, the uncertainty analysis is focused on this measurement. However, it should be noted that the analysis presented herein has been applied to the other experimental quantities and the test facility instrumentation has been designed based on this analysis. The initial starting point for the regenerator energy flow measurement (or the net cooling power measurement) is the calibration of the conductive thermal pathway that links the cold end of the test facility to the cryocooler. However, due to the non-linearity in the experimental data for the bus bar calibration, one must convert the raw experimental data, with some associated uncertainty, into a useful form via a regression analysis in order to generate the calibration curve. A typical regression analysis assumes that the independent data (e.g., the temperature difference) is error free while the dependent data (e.g., the applied heater power) has some finite experimental error. However, in this case, both of the variables have uncertainty at each data point; this must be accounted for in the regression analysis as described by Taylor (2008-09). To facilitate this, a commercial fitting software program is utilized to fit the experimental data; Silva (2007). The regression analysis is a bivariate regression and therefore includes the uncertainty in both axes via a weighting function that propagates the uncertainty from the independent variable into the prediction for the dependent variable (heater power). Using this program, the bus bar data can be fitted using any desired function; for this analysis, a 3rd order polynomial was utilized. The results from this analysis yield an expression for the heat flow (\dot{E}) as a function of the measured temperature difference given by,

$$\dot{E} = A \Delta T + B \Delta T^2 + C \Delta T^3 \quad (4)$$

where, A , B , and C are the fitted coefficients, each having a finite uncertainty. Once the calibration curve has been generated, the total uncertainty in the measurement of the regenerator

energy flow can be determined via an uncertainty propagation analysis carried out on Eqn. (4) including the uncertainty in the coefficients as well as the uncertainty in the temperature difference measurement. The uncertainty propagation is performed via partial differentiation of Eqn. (4) with respect to each of the variables and leads to:

$$U_{\dot{E}} = \left(\left(\frac{\partial \dot{E}}{\partial A} U_A \right)^2 + \left(\frac{\partial \dot{E}}{\partial B} U_B \right)^2 + \left(\frac{\partial \dot{E}}{\partial C} U_C \right)^2 + \left(\frac{\partial \dot{E}}{\partial \Delta T} U_{\Delta T} \right)^2 \right)^{\frac{1}{2}} \quad (5)$$

where $U_A, U_B,$ and $U_C,$ are the specific uncertainty values for each of the coefficients of the calibration curve and $U_{\Delta T}$ is the uncertainty in the measurement of the temperature difference. The partial differentials are relatively straightforward and therefore are not listed. A similar uncertainty analysis is performed for all of the experimental measurements as they all depend on the fitting of data to a calibration. The error bars presented for the data are designated using this uncertainty analysis.

Regenerator Energy Flow Measurement

The total energy flow towards the cold end of an isolated regenerator, also called the regenerator loss, is a combination of a net enthalpy flow related to the fact that the gas traveling towards the cold end is warmer than the gas that is returning as well as axial conduction through the various materials that make up the regenerator. The net result is an undesired heat load at the cold end (i.e., a loss of available cooling power). The regenerator is isolated from the pulse-tube component and interfaced to the commercial cryocooler using the calibrated bus bar, as shown in Figure 6. The regenerator loss is determined using the calibration curve shown in Figure 3. As it is necessary to measure the performance of the pulse-tube component at different cold end temperatures for validation purposes, the regenerator loss measurement must also be repeated at various cold end temperatures and under various flow conditions (e.g., pressure and flow amplitude) that can be reproduced during subsequent testing of the pulse tube.

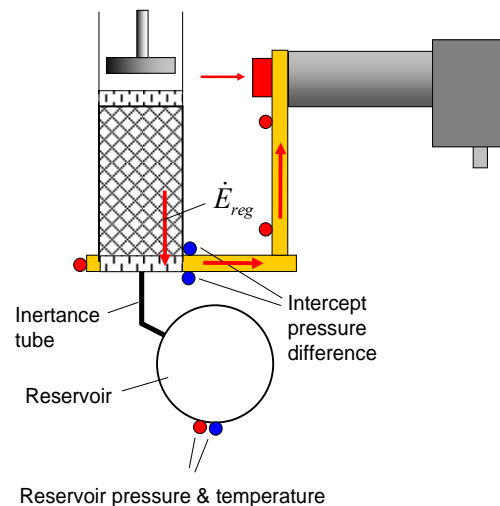


Figure 6: Illustration showing the test set-up for measurement of the regenerator loss.

The regenerator that has been tested is typical of what is used in a medium capacity PTC; the geometric specifications for the regenerator are listed in Table 1. An inertance tube was designed to provide the correct phase shift and flow rate using the model developed by Schunk (2004). For all test runs in which the regenerator energy flow was measured, the cold end temperature was maintained at 80K and an average pressure of 2.5 MPa was maintained. During actual experimental testing, the parameter which was varied was the cold end pressure ratio.

Table 1 – Regenerator Specifications

| Regenerator Parameter | Nominal Value |
|-----------------------|----------------------|
| Length (mm) | 42 |
| Diameter (mm) | 39.37 |
| Wall thickness (mm) | 0.635 |
| Porosity (-) | 0.75 |
| Packing Material | #400 Stainless Steel |

The experimental results for the regenerator energy flow measurement as function of the cold end pressure ratio are presented in Figure 7 and summarized in Table 2.

Table 2 – Regenerator test conditions

| Regenerator Parameter | PR=1.1 | PR=1.2 | PR=1.3 |
|---------------------------|--------|--------|--------|
| Cold mass flow rate (g/s) | 5.5 | 8 | 10.5 |
| Cold phase angle (deg) | -31 | -22 | -30 |
| Cold temperature (K) | 80.01 | 80.05 | 79.95 |
| Warm temperature | 298 | 299 | 301 |
| Average pressure (MPa) | 2.495 | 2.502 | 2.505 |

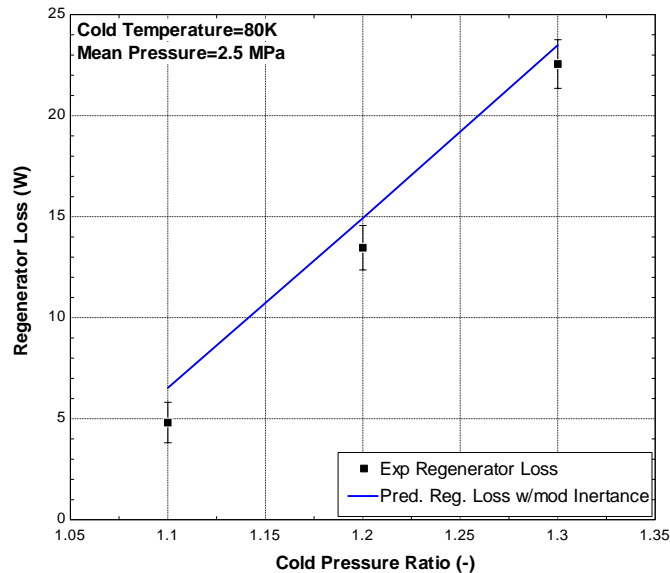


Figure 7: Plot showing the experimental results for the measurement of the regenerator loss as a function of the cold end pressure ratio with error bars; overlaid are the modeling predictions using the distributed component inertance tube model including entrance and exit effects coupled with Regen3.3 predictions for the regenerator loss.

As the results in Figure 7 show, the experimentally measured regenerator loss agrees rather well with the predictions from the inertance tube model coupled with simulations using Regen3.3 (Gary et al. 2008). The comparison to the model data was performed via determination of the mass flow rate and phase angle at the cold end using the inertance tube model taking into account the added resistance due to entrance and exit effects (calculated analytically) at each end of the inertance tube. The mass flow predicted by the inertance tube model was then compared to the actual mass flow at the cold end determined via computation of mass flow in the reservoir using Eqn (3). The results of this analysis indicated agreement to within one percent between the experimental mass flow and the mass flow predicted by the inertance tube model. The mass

flow rate and phase angle were used as inputs into the REGEN3.3; the primary inputs into the REGEN3.3 program are summarized in Table 3.

6. Proposed Future Work

Based upon the initial experimental measurements, it was realized that the mass flow meter could be improved by designing it to provide somewhat larger pressure drops that could be measured more accurately. The primary area of concern with the original mass flow meter was a much smaller signal to noise ratio than initially predicted. This problem has been alleviated via creation of a new mass flow sensor that allows for a substantial increase in the magnitude of the pressure drop across the mass flow meter. This will significantly improve the resolution of the measurement of the mass flow and phase angle which is particularly important for direct measurement of the acoustic power. Additionally, ongoing experimental work is focused on measuring the net cooling power and acoustic power flow for various CFD guided pulse-tube and flow transition designs at cold end temperatures of 60 K and 80 K.

Once the experimental measurements have been carried out, the experimental results will be utilized for comparison to the model predictions such that the overall accuracy of the CFD simulations can be determined. Subsequent modeling efforts after the experimental validation will be focused on the modeling of 4K pulse-tube and flow transitions designs. The ultimate goal of this modeling work will be the development of design charts for systems operating at 4K such that for a given set of conditions, the conversion of acoustic power flow at the cold end to useful cooling will be maximized by correct selection of the pulse-tube volume, flow transition design, and pulse-tube aspect ratio.

In the early portion of 2009, I will be joining the faculty at the Virginia Military Institute as an Assistant Professor of Mechanical Engineering. The scope of this position is that it is predominantly teaching but research is encouraged and required. As a result, I will be continuing to perform research in the cryogenics field related to cryocooler development. Specifically, I have spoken with Ray Radebaugh at NIST about working under contract during the summers performing research at NIST and have also discussed the continuation of work with my advisors Greg Nellis and Sandy Klein at the University of Wisconsin-Madison for the foreseeable future.

7. References

Rawlins, W., Radebaugh, R., Timmerhaus, K.D., "Thermal anemometry for mass flow measurements in oscillating cryogenic gas flows," *Rev. Sci. Instrum.*, Vol. 64, No. 11, (1993), pp 3229-3235.

Taylor, R.P., "Development and Experimental Validation of a Pulse-Tube Design Tool Using Computational Fluid Dynamics," *Ph.D Thesis*, The University of Wisconsin-Madison., in preparation for publication, (2008-2009).

Silva, W.P. and Cleide M.D., "LAB Fit Curve Fitting Software (Nonlinear Regression and Treatment of Data Program) V 7.2.37", online - www.labfit.net, (2007).

Schuck, L.O., "Experimental Investigation and Modeling of Inertance Tubes," *Ph.D Thesis*, The University of Wisconsin-Madison., (2004), pp 23-29.

Gary, J., O'Gallagher, A., Radebaugh, R., Huang, Y., and Marquardt, E., "REGEN3.3: User Manual," *National Institute of Standards and Technology*, (2008).